Int. J. Morphol.,
44(4):1424-1432, 2026.

Sex Estimation From Skull Measurements Using a Three-Dimensional Computed Tomography in a Contemporary Thai Population: Agreement, Reliability, and Comparative Performance with Dry Skull

Estimación del Sexo a Partir de Medidas Craneales Mediante Tomografía Computarizada Tridimensional en una Población Tailandesa Contemporánea: Concordancia, Fiabilidad y Rendimiento Comparativo con Cráneos Secos

Zhaokang Du[1,2]; Pagorn Navic[3]; Apichat Sinthubua[3]; Patison Palee[4]; Phannavich Malawan[5] & Pasuk Mahakkanukrauh[3,6]

DU, Z.; NAVIC, P.; SINTHUBUA, A.; PALEE, P.; MALAWAN, P. & MAHAKKANUKRAUH, P. Sex estimation from skull measurements using a three-dimensional computed tomography in a contemporary Thai population: Agreement, reliability, and comparative performance with dry skull. *Int. J. Morphol., 44(4)*:1424-1432, 2026.

SUMMARY: As computed tomography (CT) becomes increasingly integrated into forensic casework, metric-based sex estimation from the skull remains is a fundamental approach for biological identification. Moreover, the comparability of measurements obtained from skeletal specimens and those derived from three-dimensional (3D) CT reconstructions—and the stability of sex-estimation accuracy across measurement modalities—require further evaluation. Therefore, this study aimed to develop population-specific sex estimation models in a contemporary Thai population based on 3D-CT measurements and evaluate measurement agreement between 3D-CT and dry skull measurements. All samples were obtained from the Osteology Research and Training Center (ORTC), Faculty of Medicine, Chiang Mai University. A total of 252 individuals (126 males and 126 females) were used to develop the sex-estimation equations, and an independent holdout sample (n = 26) was used to validate the accuracy. A total of 31 measurements were obtained from both 3D-CT skull images and dry skulls. Stepwise multivariate discriminant function analysis was applied to derive sex-estimation equations, and cross-modality performance was assessed by substituting dry skull measurements into CT-based equations. The results showed that sex estimation accuracy ranged from 84.62 % to 92.31 %, with combined cranial–mandibular models demonstrating the highest accuracy. When dry skull measurements were applied to CT-derived discriminant functions, classification accuracy remained comparable across measurement modalities. Intra- and inter-observer reliability were high for both modalities (R > 0.90). Furthermore, the intra-class correlation coefficient (ICC) demonstrated excellent inter-modality agreement (0.970–0.999), with minimal absolute differences between dry skull and 3D-CT measurements. Overall, the results indicate that sex estimation remains consistent across two modalities. The high level of agreement and strong reliability support the use of CT-based osteometry as a non-invasive, standardized, and reproducible method for sex estimation in forensic contexts.

KEY WORDS: Computed tomography; Skull; Mandible; Sex estimation; 3D.

INTRODUCTION

The human skull is widely recognized as the second most sexually dimorphic skeletal element after the pelvis. Within the craniofacial complex, the mandible contributes additional measurements for sex estimation; however, its accuracy may vary compared with other skeletal regions. When combined with cranial measurements, they form a well-established basis for metric sex estimation (Gillet *et al*., 2020).

Over the past two decades, forensic anthropology has experienced a methodological transition toward digital and virtual skeletal analysis through three-dimensional (3D) imaging technologies, particularly computed tomography (CT). Multidetector computed tomography (MDCT) allows high-resolution volumetric reconstruction of skeletal structures, enabling non-destructive measurement, repeated

[1] PhD Program in Anatomy, Faculty of Medicine, Chiang Mai University, Chiang Mai, Thailand.
[2] Department of Human Anatomy, College of Basic Medicine, Dali University, Yunnan, Dali, China.
[3] Department of Anatomy, Faculty of Medicine, Chiang Mai University, Chiang Mai, Thailand.
[4] College of Arts, Media and Technology, Chiang Mai University, Chiang Mai, Thailand.
[5] Department of Radiologic Technology, Faculty of Associated Medical Science, Chiang Mai University, Chiang Mai, Thailand.
[6] Excellence Center in Osteology Research and Training Center (ORTC), Chiang Mai University, Chiang Mai, Thailand
FUNDED: This work was supported by research funding from the Faculty of Medicine, Chiang Mai University (grant no.136-2568).

Received: 2026-04-22 Accepted: 2026-06-14

analysis, and remote data sharing. These features are particularly advantageous in medico-legal contexts where direct access to remains may be restricted or preservation concerns prohibit handling (Franklin *et al*., 2013; Jerkovic´ *et al*., 2022). As a result, CT-based osteometry has become common in forensic identification research and practice. Numerous studies across diverse populations demonstrated that CT-based sex estimation can achieve high levels of accuracy, ranging from 80 % to 96 %. (Adel *et al*., 2019; Battan *et al*., 2023).

Despite these advances, equivalence between CT-derived and direct skeletal measurements should not be assumed. Previous studies often utilized independent samples rather than paired within-individual data, hindering the isolation of modality-related bias. Consequently, cross-modality measurement agreement requires explicit evaluation. Population specificity database represents another important consideration in sex estimation. Craniofacial morphology reflects genetic, environmental, and developmental influences, and discriminant functions developed for one population may not perform reliably when applied to another (Du *et al*., 2025). Although sex estimation equations have been developed for Thai skeletal collections, most models based on a single measurement modality and analyzed the cranium and mandible separately (Mahakkanukrauh *et al*., 2015; Duangchit *et al*., 2023). Moreover, paired dry bone and CT-derived datasets from the same individuals in contemporary Thai samples remain limited, restricting evaluation of cross-modality model transferability and updated population reference standards.

Therefore, this study aimed to develop population-specific sex-estimation models based on CT-derived skull measurements in a contemporary Thai population. To support their practical application, the following objectives were addressed: (i) developing sex-estimation equations based on 3D-CT measurement; (ii) evaluating intra- and inter-observer reliability for both modalities; and (iii) testing cross-modality applicability by applying skeletal measurements to 3D-CT discriminant functions.

MATERIAL AND METHOD

Ethical exemption for this study was granted by the Ethics Committee of the Faculty of Medicine, Chiang Mai University (Approval No. ANA-2568-0218).

Sample and data collection

The study examined 252 Thai adult dry skulls (126 females and 126 males), ranging in age from 26-94 years, with average ages of approximately 66 years for both sexes (males: 66.0 ± 14.2 SD; females: 65.2 ± 14.3 SD). All samples were obtained from the Osteology Research and Training Center (ORTC), Faculty of Medicine, Chiang Mai University, and were derived from individuals who died between 2006 and 2024. Skulls exhibiting fractures, deformities from other pathology, trauma, or surgical operations were excluded.

Imaging acquisition and 3D reconstruction

Each skull was scanned using a 16-row MDCT system (Activion16, Toshiba Medical System Corporation, Tokyo, Japan), positioned along the Frankfort horizontal plane. The scanning protocol included: slice thicknesses of 1.0 mm, reconstruction interval of 1.0 mm, 80 kV tube voltage, 150 mAs tube current, and 0.3s scanning time. Digital Imaging and Communications in Medicine (DICOM) format was employed to store CT images. 3D volume-rendered reconstructions were generated through threshold-based bone segmentation through Inobitec DICOM Viewer software.

Osteometric measurements

A total of 31 measurements were obtained on dry skulls and 3D-CT images, following established protocols described in previous studies (Howells, 1989; Franklin, 2005; Langley *et al*., 2016; Tunis *et al*., 2017; Zaafrane *et al*., 2018; Cappella *et al*., 2020; Swift *et al*., 2023). The description of all thirty-one measurements was given in Table I and shown in Figure 1.

For 3D-CT measurements, 3D volume-rendered reconstructions were performed using Inobitec DICOM Viewer, with bone extraction based on CT value data. The most prominent anatomical landmarks, clearly visible in both 2D and 3D views, were used for precise landmark identification. Each variable was measured three times in non-consecutive order. The mean of the three measurements then was used for analysis.

For dry skull measurements, each variable was measured using spreading and digital sliding calipers. Each measurement was repeated three times following the same protocol applied to the 3D-CT measurements.

Statistical analysis

Analyses comprised three components: (i) development of sex estimation equations using the main dataset (n = 252; 126 males, 126 females), (ii) validation of the sex estimation equations using an independent holdout sample (n = 26; 13 males, 13 females), and (iii) intra- and inter-observer reliability testing based on repeated

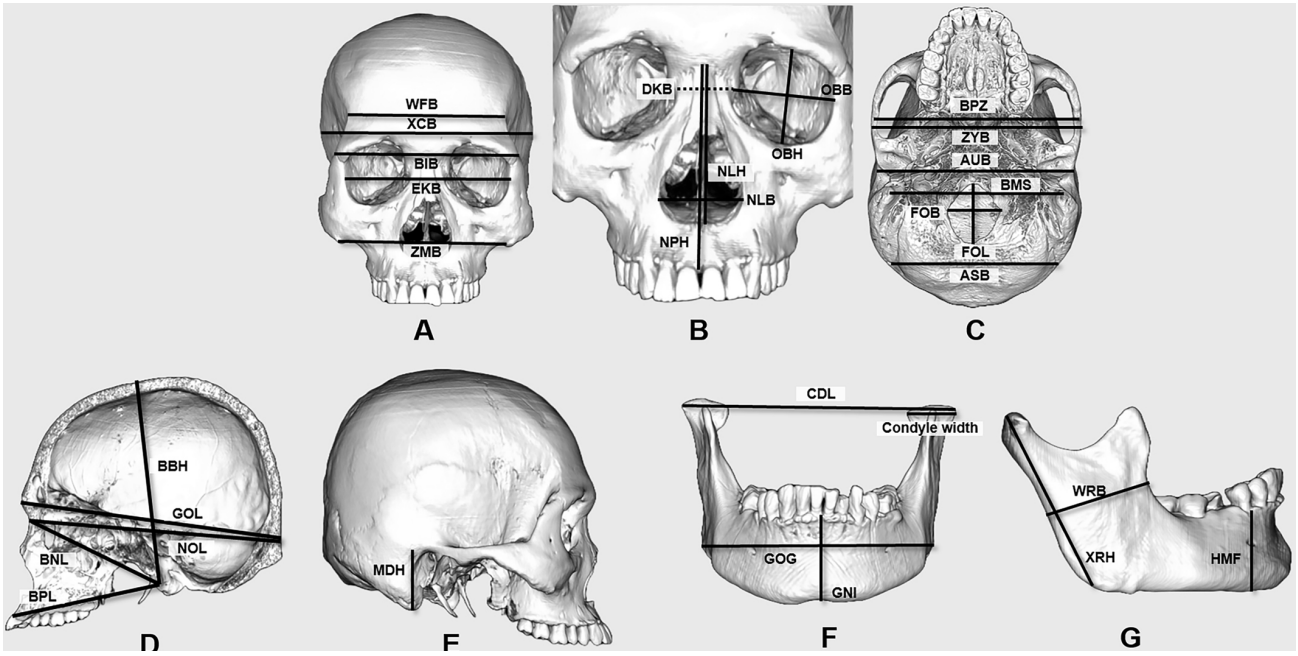


Fig. 1. Cranial and mandibular measurements used in this study. A: anterior view of the cranium B: expanded anterior view of the cranium C: inferior view of the cranium D: mid-sagittal plane of the cranium E: right lateral view of the cranium F: anterior view of the mandible G: right lateral view of the mandible.

measurements of 26 randomly selected skulls (13 males, 13 females).

Normality was assessed using the Kolmogorov–Smirnov test. Sexual dimorphism was evaluated using independent-samples t-tests for normally distributed variables and Mann–Whitney U tests otherwise. All analyses were performed with statistical significance $p < 0.05$.

Stepwise multivariate discriminant function analysis (DFA) was performed using CT-derived measurements to derive three models: a combined cranial–mandibular model, a cranial-only model, and a mandibular-only model. Leave-one-out cross-validation was used to test internal model stability. External performance was evaluated on the holdout sample.

To evaluate cross-modality applicability, the corresponding dry skull measurements were substituted into the CT-derived discriminant equations, and the accuracy was recorded. This procedure directly evaluates whether model performance transfers across measurement environments.

Intra- and inter-observer reliability were assessed using the technical error of measurement (TEM), relative TEM (rTEM), and the reliability coefficient (R) (Perini *et al*., 2005; Weinberg *et al*., 2005). Furthermore, inter-modality agreement between skeletal and CT-derived measurements was evaluated using intra-class correlation coefficients (ICC), together with magnitude-based error metrics, including mean absolute error (MAE), TEM, and rTEM.

RESULTS

Descriptive Statistics

The descriptive statistics for the dry skull and 3D-CT measurements are summarized in Tables II. All measurements showed significant sex differences ($p<0.01$) in both 3D-CT and dry skull measurement. Across modalities, males consistently exhibited higher mean values than females for all measurements.

Stepwise multivariate discriminant function analysis

Table III shows the results of the stepwise multivariate DFA based on the training dataset. Separate sex estimation equations were derived and organized into three models: (i) a combined cranial–mandibular model, (ii) a cranial-only model, and (iii) a mandibular-only model.

For the combined cranial–mandibular model, 11 out of 38 variables (GOL, NOL, ZYB, AUB, NPH, WFB, NLH, EKB, MDH, BMS, and GOG) were included in the sex-estimation function. The cranial-only model used nine cranial variables (GOL, NOL, ZYB, AUB, WFB, NLH, EKB, MDH, and BMS), while the mandibular-only model used three mandibular variables (GOG, CDL, and WRB).

Table I. Definitions of cranial and mandibular measurements.

Measurement	Abb.	Description
Cranium		
Maximum cranial length	GOL	The straight-line distance from glabella to opisthocranion in the midsagittal plane [a]
Nasio-occipital length	NOL	Maximum length in the midsagittal plane, measured from nasion [a]
Maximum cranial breadth	XCB	The maximum width of the skull perpendicular to the mid-sagittal plane wherever it is located with the exception of the inferior temporal line and the immediate area surrounds the latter [a]
Bizygomatic breadth	ZYB	The maximum breadth across the zygomatic arches, wherever found, perpendicular to the mid-sagittal plane [a]
Basion-bregma height	BBH	The distance from basion to bregma [a]
Cranial base length	BNL	The distance from nasion to basion [a]
Basion-prosthion length	BPL	The distance from basion to prosthion [a]
Biauricular breadth	AUB	The least exterior breadth across the roots of the zygomatic processes [a]
Nasion-prosthion height	NPH	The distance from nasion to prosthion [a]
Minimum frontal breadth	WFB	The distance between the right and left frontotemporale [a]
Upper facial breadth	BIB	The distance between the right and left frontomalare temporale [b, c]
Nasal height	NLH	The average height from nasion to the lowest point on the border of the nasal aperture on either side [a]
Nasal breadth	NLB	The maximum breadth of the nasal aperture [a]
Orbital breadth	OBB	The distance from dacryon to ectoconchion [a]
Orbital height	OBH	The distance between the superior and inferior orbital margins perpendicular to orbital breadth and bisecting the orbit into equal medial and lateral halves [a]
Biorbital breadth	EKB	The distance from left to right ectoconchion [a]
Interorbital breadth	DKB	The distance between right and left dacryon [a]
Foramen magnum length	FOL	The mid-sagittal distance from the most anterior point on the foramen magnum margin to opisthion [a]
Foramen magnum breadth	FOB	The distance between the lateral margins of the foramen magnum at the point of greatest lateral curvature [a]
Mastoid height	MDH	The direct distance between porion and mastoidale [a]
Biasterionic breadth	ASB	Straight-line distance from left to right asterion [a]
Bimaxillary breadth	ZMB	Breadth across the maxillae, from the left to right zygomaxillare anterior [a]
Bimastoïdale	BMS	Direct distance between the two mastoïdale [d, e]
Bizygotemporal breadth	BPZ	Direct length between both zygotemporale [b, c]
Mandible		
Chin height	GNI	Direct distance between infradentale and gnathion [f]
Height of the mandibular body	HMF	Distance between alveolar process to inferior mandible border at the mental foramen [f]
Bigonial width	GOG	Direct distance between right gonion and left gonion [f]
Bicondylar breadth	CDL	Direct distance between right condylion and left condylion [f]
Minimum ramus breadth	WRB	Least distance between the most anterior and the most posterior border of the ramus [f]
Maximum ramus height (Right, Left)	XRH	Direct distance between gonion and condylion superior [f]
Condyle width	-	The distance between most lateral and medial points of the condyle head [g]

a Langley *et al*. (2016), b Swift *et al*. (2023), c Franklin (2005), d Zaafrane *et al*. (2018), e Howells (1989), f Cappella *et al*. (2020), g Tunis *et al*. (2017).

Table II. Descriptive statistics for 3D-CT and dry skull measurements.

Variable	N	Male		N	Female		Sex different *p*-value
		3D-CT	Dry skull		3D-CT	Dry skull	
		Mean ± SD	Mean ± SD		Mean ± SD	Mean ± SD	
MCL	126	171.93 ± 6.58	171.50 ± 6.57	126	163.11 ± 5.65	162.60 ± 5.67	<0.001*
NOL	126	168.72 ± 6.48	168.30 ± 6.51	126	160.46 ± 5.72	159.95 ± 5.74	<0.001*
MCB	126	144.15 ± 5.75	143.80 ± 5.74	126	139.22 ± 5.41	138.81 ± 5.41	<0.001*
BZB	126	133.75 ± 4.64	133.66 ± 4.87	126	124.97 ± 5.00	124.59 ± 4.99	<0.001*
BBH	126	137.90 ± 4.94	137.32 ± 4.98	122	131.87 ± 4.31	131.30 ± 4.28	<0.001*
CBL	126	99.82 ± 3.60	99.30 ± 3.61	126	93.71 ± 3.74	93.17 ± 3.75	<0.001*
BPL	123	95.35 ± 5.34	95.14 ± 5.34	125	91.45 ± 5.38	91.13 ± 5.41	<0.001*
BAB	126	127.06 ± 4.84	127.14 ± 4.86	126	120.57 ± 4.73	120.63 ± 4.72	<0.001*
NPH	123	69.54 ± 4.80	69.53 ± 4.83	125	64.45 ± 4.65	64.41 ± 4.60	<0.001*
MFB	126	92.97 ± 4.98	92.96 ± 4.97	126	90.16 ± 3.92	90.14 ± 3.92	<0.001*
UFB	126	105.44 ± 3.98	105.44 ± 3.97	126	100.80 ± 4.13	100.80 ± 4.14	<0.001*
NSH	125	55.08 ± 3.11	55.03 ± 3.08	126	50.24 ± 2.54	50.24 ± 2.51	<0.001*
NSB	126	27.31 ± 1.97	27.20 ± 1.95	126	25.87 ± 1.77	25.78 ± 1.67	<0.001*
ORB	126	40.52 ± 1.81	40.59 ± 1.77	126	38.83 ± 1.75	38.89 ± 1.74	<0.001*
ORH	126	34.54 ± 1.95	34.48 ± 1.94	126	33.29 ± 1.68	33.24 ± 1.65	<0.001*
BOB	126	98.65 ± 3.77	98.66 ± 3.81	126	94.72 ± 3.92	94.72 ± 3.96	<0.001*
IOB	126	20.42 ± 2.27	20.33 ± 2.26	126	19.49 ± 2.08	19.43 ± 2.07	0.001*
FML	126	35.56 ± 2.57	35.52 ± 2.54	126	33.53 ± 2.36	33.45 ± 2.34	<0.001*
FMB	126	30.75 ± 1.85	30.64 ± 1.84	126	29.13 ± 2.00	29.02 ± 1.96	<0.001*
MSH	126	32.01 ± 3.35	32.02 ± 3.34	126	28.00 ± 3.00	27.93 ± 2.94	<0.001*
BASB	126	109.30 ± 4.68	109.33 ± 4.66	126	106.49 ± 4.46	106.47 ± 4.46	<0.001*
BXB	126	99.23 ± 4.89	99.14 ± 4.79	126	93.53 ± 4.53	93.55 ± 4.51	<0.001*
BMSD	125	107.81 ± 4.19	107.80 ± 4.20	126	102.06 ± 4.74	102.04 ± 4.75	<0.001*
BZTB	125	127.05 ± 4.63	127.10 ± 4.66	126	119.20 ± 4.69	119.10 ± 4.71	<0.001*
CIH	126	29.99 ± 5.00	30.05 ± 5.03	125	27.27 ± 5.10	27.41 ± 5.11	<0.001*
HMB	126	28.71 ± 4.71	28.76 ± 4.73	125	26.54 ± 4.68	26.48 ± 4.63	<0.001*
BGTH	126	97.86 ± 5.80	98.00 ± 5.94	125	90.91 ± 5.43	90.84 ± 5.45	<0.001*
BCTH	124	123.66 ± 5.43	123.76 ± 5.47	125	116.50 ± 5.23	116.58 ± 5.22	<0.001*
MRB	126	34.04 ± 2.81	33.97 ± 2.83	126	31.74 ± 2.68	31.64 ± 2.68	<0.001*
MRH	126	62.34 ± 4.78	62.34 ± 4.77	126	56.17 ± 3.54	56.17 ± 3.57	<0.001*
Condyle width	126	20.50 ± 2.02	20.63 ± 2.02	126	18.52 ± 1.75	18.60 ± 1.73	<0.001*

*Indicates statistically significant sex differences ($p < 0.05$) in both modalities.

Classification accuracy

Table III also provides classification accuracy rates from both the original and the cross-validation analysis. Holdout validation results are presented in Table IV. Overall accuracy ranged from 84.62 % to 92.31 %. The highest accuracy was achieved using the combined cranial and mandibular variables, yielding 92.31 % for the dry skull and 3D-CT measurements. The cranial-only model was the next most accurate, with accuracies of 88.46 % and 92.31 %, respectively, followed by the mandibular-only model, which produced accuracies of 84.62 % for both measurement methods. When dry skull measurements were entered into the CT-derived discriminant functions, classification accuracy remained comparable across modalities, indicating stable model performance across modalities despite minor measurement variation.

Consistency of dry skull and 3D-CT measurements

The MAE between modalities were minimal across variables, typically below 1 mm, with corresponding TEM and rTEM values indicating low measurement discrepancy. The ICC values were quite high, ranging from 0.970 to 0.999. Minor increases in measurement discrepancy were observed in variables involving curved surfaces or less sharply defined landmarks.

Intra- and inter-observer reliability

Both skeletal and CT-derived measurements demonstrated low TEM and rTEM values with reliability coefficients generally exceeding 0.90, indicating high reproducibility and measurement reliability.

Table III. Discriminant function coefficients and classification accuracy (%) derived from stepwise multivariate DFA using 3D-CT measurements for sex estimation.

Function	Equation	Group centroid		% original grouped			% cross-validated		
		M	F	Overall	M	F	Overall	M	F
1	Discriminant score = -28.452 + (0.269xGOL) + (-0.204xNOL) + (0.233xZYB) + (-0.128xAUB) + (-0.047xNPH) + (-0.071xWFB) + (0.158xNLH) + (-0.107xEKB) + (0.109xMDH) + (0.061xBMS) + (0.049xGOG)	1.465	-1.477	94	93.7	94.4	92.1	91.3	92.9
2	Discriminant score = -28.285 + (0.289xGOL) + (-0.223xNOL) + (0.240xZYB) + (-0.130xAUB) + (-0.055xWFB) + (0.126xNLH) + (-0.098xEKB) + (0.104xMDH) + (0.061xBMS)	1.399	-1.399	91.6	91.1	92.1	90.8	90.3	91.3
3	Discriminant score = -24.662 + (0.054xGOG) + (0.092xCDL) + (0.145xWRB)	0.98	-0.98	83.1	84.7	81.6	83.1	84.7	81.6

Function 1 = a combined cranial–mandibular model; Function 2 = a cranial-only model; Function 3 = a mandibular-only model.

Table IV. Test of stepwise multivariate DFA on the 26 holdout skeletons.

Function	Accuracy (%)	
	3D-CT	Dry skull
Function 1: a combined cranial–mandibular model	92.31	92.31
Function 2: a cranial-only model	92.31	88.46
Function 3: a mandibular-only model	84.62	84.62

DISCUSSION

Measurement agreement between modalities

Intra- and inter-observer reliability yielded excellent reproducibility and repeatability (R > 0.90). Agreement between modalities demonstrated ICC values ranging from 0.970 to 0.999, supported by small absolute differences and low magnitude-based error metrics. These findings are consistent with previous studies reporting high reliability of CT-based cranial and mandibular measurements both within single observers and across different observers (Zaafrane *et al*., 2018; Adel *et al*., 2019; Battan *et al*., 2023; Hoshioka *et al*., 2025).

Most directly, Jerkovic *et al*. (2022), reported intra-observer TEM values of approximately 0.65–0.67 mm and rTEM around 1.15–1.25 % for cranial measurements obtained from dry skulls and CT reconstructions. A comparable sensitivity pattern was observed in the present study, where slightly higher discrepancies occurred in variables associated with curved surfaces or less clearly defined landmarks. However, these deviations remained small and within acceptable forensic limits. Consistent with this observation, craniometric measurements obtained from both dry bones and CT reconstructions were still accurate and reliable (Franklin *et al*., 2013; Jerkovic *et al*., 2022).

Sexual dimorphism and variable contribution

As expected, males consistently exhibited larger values than females, reflecting well-established differences in craniofacial robusticity and overall skeletal size. Several cranial and mandibular variables—specifically ZYB, NOL, GOL, BBH, AUB, and BMS in the cranium, and GOG, CDL, and WRB in the mandible—were identified as strong predictors of sex classification in the present study and are consistent with those reported in previous studies.

Variables such as ZYB, BNL, GOL, and BMS, along with vertical cranial measures including BBH, were consistently identified as well-established indicators of sex (Zaafrane *et al*., 2018; Adel *et al*., 2019; Cappella *et al*., 2020; Gillet *et al*., 2020; Battan *et al*., 2023; Swift *et al*., 2023; Hoshioka *et al*., 2025). Likewise, mandibular variables including GOG, CDL, and WRB also demonstrated good discriminatory power in previous studies (Franklin *et al*., 2008; Gamba *et al*., 2016; Álvarez Villanueva *et al*., 2017; Tunis *et al*., 2017; Cappella *et al*., 2020; Fakher *et al*., 2020; Gillet *et al*., 2020). Their consistent selection across different populations and measurement methods suggests that these variables represent stable patterns of craniofacial sexual dimorphism.

Comparison of classification accuracy with previous studies

The classification accuracy observed in the present study was comparable to, and in some cases exceeded, those reported for diverse populations, including African (Franklin *et al*., 2008), Italian (Cappella *et al*., 2020), and Mexican (Álvarez Villanueva *et al*., 2017) samples. Overall, our model achieved accuracies ranging from 84.62 % to 92.31 %, which falls well within the ranges reported in previous studies, where cranial-based methods typically achieve accuracies of 77.5–96.3 % (Zaafrane *et al*., 2018; Gillet *et al*., 2020; Battan *et al*., 2023; Swift *et al*., 2023; Hoshioka *et al*., 2025) and mandibular-based methods have ranged from 72.9 % to 94.7 % (Gamba *et al*., 2016; Tunis *et al*., 2017; Fakher *et al*., 2020).

When compared with previous studies in Thai populations, the classification accuracy in the present study was higher, particularly when cranial and mandibular variables were analyzed together. Mahakkanukrauh *et al*. (2015), reported cranial-only discriminant models achieving accuracies exceeding 90 %, whereas Duangchit *et al*. (2023), reported performance for mandibular-only approaches (76 % dry bone and 70 % radiographic assessments). These previous studies provide important benchmarks but differ from the present study in sample size, modality approaches, or the development of models. In contrast, the present study examined paired dry skull and 3D-CT measurements from the same individuals within a contemporary Thai dataset, allowing direct evaluation of consistency between modalities. The model achieved classification accuracies ranging from 84.62 % to 92.31 %. These results highlight the advantage of integrating cranial and mandibular measurements and provide updated population-specific reference data for forensic applications.

Implications for forensic anthropology

CT-based approach is particularly valuable in cases involving inaccessible remains, as well as in mass-disaster scenarios requiring rapid, non-destructive assessment (Crebert *et al*., 2025). Given the widespread availability of CT imaging in medico-legal and hospital settings, integrating 3D-CT into routine forensic anthropological practice may improve accessibility, reduce examination time, and minimize damage to skeletal material. At the same time, direct examination of dry skulls remains important for detailed qualitative assessment. Although the CT data in the present study were derived from dry skulls, the high level of measurement consistency observed provides a useful baseline for applying CT-based osteometry in situations where direct access or handling of skeletal remains is limited.

Limitations and future directions

The CT data were obtained using standard clinical scanning parameters, which, although appropriate for routine imaging, may not provide the spatial resolution achievable with high-dose, thin-slice protocols used for dry bone scanning. Variability in reconstruction algorithms and user-defined rendering settings may also influence landmark visualization. Future studies should aim to expand sample sizes, establish standardized protocols for CT-based measurement, evaluate consistency across different imaging platforms and reconstruction software, and explore the use of machine learning and automated or artificial intelligence-assisted landmark identification to further enhance measurement reproducibility (Noel *et al*., 2024).

CONCLUSION

Stepwise discriminant models achieved high holdout classification accuracy (84.62–92.31 %). Paired dry skull and CT-derived measurements demonstrated strong agreement and high reproducibility in a contemporary Thai sample. Comparable outcomes under cross-modality substitution indicate that sex-estimation equations remain functionally stable despite minor metric variation, supporting operational compatibility between direct and CT-derived

osteometry under standardized protocols. These data provide updated population-specific reference models and a paired-modality framework for evaluating measurement transferability in forensic practice. Future research should expand demographic representation, evaluate modality performance across imaging platforms and scanning parameters, and investigate the use of machine learning and automated or artificial intelligence to further enhance accuracy and reproducibility.

ACKNOWLEDGEMENTS

The authors gratefully acknowledge support from the Excellence in Osteology Research and Training Center (ORTC), Chiang Mai University.

DU, Z.; NAVIC, P.; SINTHUBUA, A.; PALEE, P.; MALAWAN, P. & MAHAKKANUKRAUH, P. Estimación del sexo a partir de medidas craneales mediante tomografía computarizada tridimensional en una población tailandesa contemporánea: Concordancia, fiabilidad y rendimiento comparativo con cráneos secos. *Int. J. Morphol., 44(4)*:1424-1432, 2026.

RESUMEN: A medida que la tomografía computarizada (TC) se integra cada vez más en la práctica forense, la estimación del sexo basada en medidas de restos craneales sigue siendo un enfoque fundamental para la identificación biológica. Además, la comparabilidad entre las medidas obtenidas de especímenes óseos y las derivadas de reconstrucciones de TC tridimensional (3D)—así como la estabilidad de la precisión en la estimación del sexo entre las distintas modalidades de medición—requieren una evaluación adicional. Por ello, este estudio tuvo como objetivo desarrollar modelos de estimación del sexo específicos para una población tailandesa contemporánea, basados en medidas de TC-3D, y evaluar la concordancia de las medidas entre la TC-3D y el cráneo seco. Todas las muestras se obtuvieron del Centro de Investigación y Formación en Osteología (ORTC) de la Facultad de Medicina de la Universidad de Chiang Mai. Se utilizó un total de 252 individuos (126 hombres y 126 mujeres) para desarrollar las ecuaciones de estimación del sexo, y una muestra independiente de validación (n = 26) para comprobar la precisión. Se obtuvieron 31 medidas tanto de las imágenes craneales por TC-3D como de los cráneos secos. Se aplicó un análisis de función discriminante multivariante por pasos (*stepwise*) para derivar las ecuaciones de estimación del sexo, y se evaluó el rendimiento entre modalidades sustituyendo las medidas de cráneo seco en las ecuaciones basadas en TC. Los resultados mostraron que la precisión en la estimación del sexo osciló entre el 84,62 % y el 92,31 %, siendo los modelos combinados craneomandibulares los que demostraron mayor precisión. Al aplicar las medidas de cráneo seco a las funciones discriminantes derivadas de la TC, la precisión de la clasificación se mantuvo comparable entre las modalidades de medición. La fiabilidad intra e inter observador fue alta para ambas modalidades (R > 0,90). Asimismo, el coeficiente de correlación intraclase (CCI) demostró una excelente concordancia entre modalidades (0,970–0,999), con diferencias absolutas mínimas entre las medidas de cráneo seco y las de TC-3D. En conjunto, los resultados indican que la estimación del sexo se mantiene consistente entre ambas modalidades. El alto grado de concordancia y la elevada fiabilidad respaldan el uso de la osteometría basada en TC como un método no invasivo, estandarizado y reproducible para la estimación del sexo en contextos forenses.

PALABRAS CLAVE: Tomografía computarizada; Cráneo; Mandíbula; Estimación del sexo; 3D.

REFERENCES

Adel, R.; Ahmed, H. M.; Hassan, O. A. & Abdelgawad, E. A. Assessment of craniometric sexual dimorphism using multidetector computed tomographic imaging in a sample of Egyptian population. *Am. J. Forensic Med. Pathol., 40(1)*:19-26, 2019.

Álvarez Villanueva, E.; Menéndez Garmendia, A.; Torres, G.; Sánchez-Mejorada, G. & Gómez-Valdés, J. A. Gender assessment using the mandible in the Mexican population. *Span. J. Leg. Med., 43(4)*:146-54, 2017.

Battan, S. K.; Sharma, M.; Gakhar, G.; Garg, M.; Singh, P. & Jasuja, O. Cranio-facial bones evaluation based on clinical CT data for sex determination in Northwest Indian population. *Leg. Med., 64*:102292, 2023.

Cappella, A.; Gibelli, D.; Vitale, A.; Zago, M.; Dolci, C.; Sforza, C. & Cattaneo, C. Preliminary study on sexual dimorphism of metric traits of cranium and mandible in a modern Italian skeletal population and review of population literature. *Leg. Med., 44*:101695, 2020.

Crebert, I.; Seckiner, D.; Nickson, R.; Berezowski, V. & Mallett, X. A comparative analysis of computed tomography, photogrammetry, and structured light scanning for biological sex estimation in forensic anthropology – a review. *Sci. Justice, 65(4)*:101263, 2025.

Du, Z.; Navic, P. & Mahakkanukrauh, P. Sex, stature, and age estimation from skull using computed tomography images: current status, challenges, and future perspectives. *Med. Sci. Law, 65(4)*:321-38, 2025.

Duangchit, S.; Boonthai, W.; Sindecharak, T.; Munkong, W.; Tangsrisakda, N.; Poodendaen, C. & Srisen, K. Sex determination from the mandible of the Northeastern Thai population: compared between conventional and radiographic measurements. *Srinagarind Med. J., 38(6)*:578-88, 2023.

Fakher, M. A.; Owayda, A.; Al-Assaf, M.; Hamadah, O.; Abdul-Hak, M. & Nofal, H. Mandibular sexual dimorphism analysis in CBCT scans in a Syrian sample. *Cumhur. Dent. J., 23(2)*:124-8, 2020.

Franklin, D. *Cranial Variation in Southern Africa: A Series of Inter-Landmark and Three-Dimensional Multivariate Morphometric Studies*. Perth, University of Western Australia, 2005.

Franklin, D.; Cardini, A.; Flavel, A.; Kuliukas, A.; Marks, M. K.; Hart, R.; Oxnard, C. & O'Higgins, P. Concordance of traditional osteometric and volume-rendered MSCT interlandmark cranial measurements. *Int. J. Legal Med., 127(2)*:505-20, 2013.

Franklin, D.; O'Higgins, P.; Oxnard, C. E. & Dadour, I. Discriminant function sexing of the mandible of Indigenous South Africans. Forensic *Sci. Int., 179(1)*:84.e1-5, 2008.

Gamba, T. O.; Alves, M. C. & Haiter-Neto, F. Mandibular sexual dimorphism analysis in CBCT scans. *J. Forensic Leg. Med., 38*:106-10, 2016.

Gillet, C.; Costa-Mendes, L.; Rérolle, C.; Telmon, N.; Maret, D. & Savall, F. Sex estimation in the cranium and mandible: a multislice computed tomography (MSCT) study using anthropometric and geometric morphometry methods. *Int. J. Legal Med., 134(2)*:823-32, 2020.

Hoshioka, Y.; Torimitsu, S.; Makino, Y.; Yajima, D.; Chiba, F.; Yamaguchi, R.; Inokuchi, G.; Motomura, A.; Tsuneya, S. & Iwase, H. Sex estimation from skull measurements of a contemporary Japanese population using three-dimensional computed tomography images. *Int. J. Legal Med., 139(1)*:383-91, 2025.

Howells, W. W. Skull Shapes and the Map: Craniometric Analyses in the Dispersion of Modern Homo. *Papers of the Peabody Museum of Archaeology and Ethnology*, Vol. 79. Cambridge, Harvard University, 1989.

Jerkovic, I.; Basic, Z.; Baresa, T.; Kresic, E.; Adamic Hadzic, A.; Dolic, K.; Cavar Boric, M.; Budimir Mrsic, D.; Cavka, M.; Slaus, M.; *et al*. The repeatability of standard cranial measurements on dry bones and MSCT images. *J. Forensic Sci., 67(5)*:1938-47, 2022.

Langley, N. R.; Jantz, L. M.; Ousley, S. D.; Jantz, R. L. & Milner, G. *Data Collection Procedures for Forensic Skeletal Material 2.0*. Knoxville, University of Tennessee and Lincoln Memorial University, 2016.

Mahakkanukrauh, P.; Sinthubua, A.; Prasitwattanaseree, S.; Ruengdit, S.; Singsuwan, P.; Praneatpolgrang, S. & Duangto, P. Craniometric study for sex determination in a Thai population. *Anat. Cell Biol., 48(4)*:275-83, 2015.

Noel, L.; Fat, S. C.; Causey, J. L.; Dong, W.; Stubblefield, J.; Szymanski, K.; Chang, J. H.; Wang, P. Z.; Moore, J. H.; Ray, E.; *et al*. Sex classification of 3D skull images using deep neural networks. *Sci. Rep., 14(1)*:13707, 2024.

Perini, T. A.; Oliveira, G. L. de; Ornellas, J. de S. & Oliveira, F. P. de. Technical error of measurement in anthropometry. *Rev. Bras. Med. Esporte, 11*:81-5, 2005.

Swift, L.; Obertova, Z.; Flavel, A.; Murray, K. & Franklin, D. Estimation of sex from cranial measurements in an Australian population. *Aust. J. Forensic Sci., 55(6)*:755-70, 2023.

Tunis, T. S.; Sarig, R.; Cohen, H.; Medlej, B.; Peled, N. & May, H. Sex estimation using computed tomography of the mandible. *Int. J. Legal Med., 131(6)*:1691-700, 2017.

Weinberg, S. M.; Scott, N. M.; Neiswanger, K. & Marazita, M. L. Intraobserver error associated with measurements of the hand. *Am. J. Hum. Biol., 17(3)*:368-71, 2005.

Zaafrane, M.; Ben Khelil, M.; Naccache, I.; Ezzedine, E.; Savall, F.; Telmon, N.; Mnif, N. & Hamdoun, M. Sex determination of a Tunisian population by CT scan analysis of the skull. *Int. J. Legal Med., 132(3)*:853-62, 2018.

Corresponding author:
Prof. Pasuk Mahakkanukrauh, MD.
Research Cluster in Osteology Research and Training Center (ORTC)
Chiang Mai University
Chiang Mai 50200
THAILAND

E-mail: pasuk034@gmail.com